

# Evolving Multi-Channel Confidence-Aware Activation Functions for Missing Data with Channel Propagation

Naeem Shahabi Sani  
shahabi@ou.edu  
University of Oklahoma  
Norman, Oklahoma, USA

Ferial Najiantabriz  
ferial@ou.edu  
University of Oklahoma  
Norman, Oklahoma, USA

Shayan Shafaei  
shayan.shafaei@ou.edu  
University of Oklahoma  
Norman, Oklahoma, USA

Dean F. Hougen  
hougen@ou.edu  
University of Oklahoma  
Norman, Oklahoma, USA

## Abstract

Learning in the presence of missing data can result in biased predictions and poor generalizability, among other difficulties, which data imputation methods only partially address. In neural networks, activation functions significantly affect performance yet typical options (e.g., ReLU, Swish) operate only on feature values and do not account for missingness indicators or confidence scores. We propose *Three-Channel Evolved Activations* (3C-EA), which we evolve using GP to produce multivariate activation functions  $f(x, m, c)$  in the form of trees that take (i) the feature value  $x$ , (ii) a missingness indicator  $m$ , and (iii) an imputation confidence score  $c$ . To make these activations useful beyond the input layer, we introduce *ChannelProp*, an algorithm that deterministically propagates missingness and confidence values via linear layers based on weight magnitudes, retaining reliability signals throughout the network. We evaluate 3C-EA and ChannelProp on datasets with natural and injected (MCAR/MAR/MNAR) missingness at multiple rates under identical preprocessing and splits. Results indicate that integrating missingness and confidence inputs into the activation search improves classification performance under missingness.

## Keywords

Genetic Programming, Missing Data, Activation Functions, Confidence Propagation, Neural Networks

## 1 Introduction

In real-world machine learning applications, data is rarely complete [15]. Missing values are common in fields such as medical informatics, finance, and sensor networks, requiring preprocessing techniques such as imputation or masking [4, 15, 23]. Although these strategies allow models to work with incomplete information, they frequently obscure an essential contrast between observed data and imputed projections [26]. Traditional neural networks intensify this problem by depending on fixed scalar activation functions (e.g., ReLU, Swish, ELU) that function only on the feature value  $x$  and fail to clearly distinguish between high-confidence observations and low-confidence imputations.

A common strategy for addressing missing data is to use missingness masks or indicators as secondary input features. This enables the network to use missingness information; nevertheless, the nonlinear transformations remain unaltered, and any reliability information must be inferred implicitly via linear weights [5]. Consequently, designing nonlinear behaviors that explicitly respond to data quality remains a significant challenge.

Neuroevolution provides a structured solution by allowing the automatic identification of neural components that are challenging to design by hand [21]. Previous research has demonstrated

that evolutionary search may identify enhanced scalar activation functions  $f(x)$  and effectively navigate complex function spaces via genetic programming (GP) [5, 12]. Nonetheless, current activation function searches are primarily limited to scalar inputs and are unable to directly utilize data-quality information. This work presents *Three-Channel Evolved Activations* (3C-EA), which expand activation evolution to multivariate computation trees represented as  $f(x, m, c)$ , where  $x$  symbolizes the feature value,  $m$  acts as a binary missingness indicator, and  $c$  shows an imputation confidence score. In our approach, confidence is set to 1 for observed values and decreased for imputed values according to feature-specific missingness rates derived from the training data.

To improve multi-channel activations in deep networks, we present *ChannelProp*, a deterministic propagation rule that communicates missingness and confidence via linear layers by employing normalized absolute weight values. This guarantees that reliability information gets transformed together with feature values instead of being eliminated post-input layer. Accordingly, evolved activations can locally modify their responses, such as by diminishing activations in low-confidence scenarios or altering regimes in the absence of inputs. We evaluate the proposed method on datasets with natural missing values and on initially full datasets with intentionally created missingness under missing completely at random, missing at random, and missing not at random (MCAR, MAR, and MNAR, respectively) methods [15]. Performance is evaluated against standard fixed activation baselines (ReLU, Swish, LeakyReLU, ELU) with identical preprocessing procedures and identical train, validation, and test splits.

**Contributions.** (i) We present a GP-based system for evolving multivariate activation functions that clearly depend on feature values, missingness indicators, and confidence scores; (ii) We introduce ChannelProp, a deterministic approach to propagating reliability information across linear layers; (iii) We illustrate via extensive experiments that integrating data-quality information into the activation search space results in measurable performance enhancements, especially in scenarios of structured and value-dependent missingness.

## 2 Related Work

### 2.1 Missing Data Handling

Missing data has been widely studied in machine learning [8, 11, 17, 24, 25, 27]. Traditional methods use single or multiple imputation based on assumptions such as MCAR, MAR, and MNAR [15, 22]. Mean imputation and model-based methods like expectation-maximization and k-nearest neighbors are common strategies. They are fast to run but may hide uncertainty [4, 23]. Recent research integrates missingness markers as supplementary inputs, enabling

models to condition on observedness data [6, 14]. Evolutionary methods have been investigated for missing-data issues, primarily via imputation-based optimization [3, 16]. Nevertheless, most of current methods consider activation functions as fixed factors, constraining the capacity of nonlinear transformations to directly adjust to data dependability [1, 5, 7].

## 2.2 Evolved Neural Activation Functions

Activation functions are a crucial part of neural network performance [7, 9, 20]. Although researchers have long depended on fixed nonlinearities, the trend has been towards automated discovery to move past the shortcomings of manually designed functions [13].

Ramachandran et al. [20] applied reinforcement learning to automatically identify enhanced scalar activation functions, whereas later researchers have employed evolutionary computation to expand the search space. Bingham et al. [5] used (GP) to evolve scalar activation functions in a tree-based search space, showing improvements over ReLU, while Parisi et al. [18] used genetic algorithms to optimize nonlinear operators in a predefined activation search space.

Our method expands on the evolutionary line of research by including the discovery of evolving activation functions from scalar nonlinearities to multivariate, reliability-aware activations that work together on feature values, missingness indicators, and confidence signals.

## 3 Method

### 3.1 Problem setup and three-channel inputs

Let  $\mathcal{D} = \{(\mathbf{x}^{(i)}, y^{(i)})\}_{i=1}^n$  represent a tabular classification dataset comprised of  $d$  features, where  $\mathbf{x}^{(i)} \in \mathbb{R}^d$  may include missing values and  $y^{(i)}$  represents the class label. Standard multilayer perceptrons (MLPs) often employ a fixed scalar nonlinearity  $g(z)$  (e.g., ReLU, Swish, ELU) for each pre-activation  $z$ , treating both observed values and imputed estimations similarly.

We present explicit reliability information to the nonlinearity by creating three channels for each feature: (i) an imputed value channel  $\tilde{x}$ , (ii) a missingness indicator  $m \in [0, 1]$ , and (iii) a confidence score  $c \in [0, 1]$ . In the input layer,  $m \in \{0, 1\}$  indicates the absence of a feature; in subsequent layers,  $m$  transforms into a soft missingness probability through deterministic propagation (Section 3.3). Our purpose is to create an unique multivariate activation function

$$f(\tilde{x}, m, c), \quad (1)$$

through GP, and to apply this activation in each hidden layer of a three-channel MLP (3C-MLP). This enables the nonlinearity to adjust responses according to the degree of missing data and reliability.

### 3.2 Channel Construction: Imputation, Missingness, and Confidence

Each dataset handles missing values via an intentional three-channel representation constructed before network training. Let  $\mathbf{X} \in \mathbb{R}^{n \times d}$  represent the the feature matrix after missingness injection (when applicable). We derive the following channels.

**Imputed value channel.** Missing entries are imputed using feature-specific methods calculated only from the training set. Let  $\mu_j$  represent the mean of feature  $j$  calculated from the observed training data. All missing values in the training, validation, and test subsets are substituted with  $\mu_j$ . This approach prevents data leakage while ensuring a uniform numeric input  $\tilde{x}$  for the next processing step.

**Missingness channel.** A binary missingness mask  $m$  is generated concurrently with imputation, where  $m_{ij} = 1$  indicates that feature  $j$  of sample  $i$  is missing, while  $m_{ij} = 0$  indicates its presence. Although  $m$  is binary at the input layer, it turns into a soft missingness probability in subsequent layers via deterministic propagation (Section 3.3).

**Confidence Channel.** To checking the reliability of imputed values, we provide a confidence score  $c \in [0, 1]$  to each feature. For observed entries, confidence is determined as  $c_{ij} = 1$ . For missing entries, confidence reduces corresponding with the feature-specific missing rate derived from the training data. Let

$$r_j = \frac{1}{n_{\text{train}}} \sum_{i=1}^{n_{\text{train}}} m_{ij}$$

represent the proportion of missing values in feature  $j$  inside the training dataset. For missing entries, confidence is defined as

$$c_{ij} = \max(\tau, 1 - r_j),$$

where  $\tau$  is a minimal lower threshold (set at  $\tau = 0.1$  in all tests) to avoid numerical collapse. This creates a dataset-driven, feature-specific confidence heuristic that indicates the relative reliability of imputed values without adding extra learned factors.

### 3.3 ChannelProp: Deterministic Propagation of Reliability Metadata

To enable reliability-aware activations beyond the input layer, missingness and confidence information must be propagated through linear transformations. Standard mask-as-feature approaches provide no such mechanism, causing reliability metadata to vanish after the first layer. We address this limitation with *ChannelProp*, a deterministic propagation rule that transports missingness and confidence alongside feature values across linear layers. Let  $\mathbf{c}_{\text{in}} \in [0, 1]^{d_{\text{in}}}$  and  $\mathbf{m}_{\text{in}} \in [0, 1]^{d_{\text{in}}}$  denote the confidence and missingness vectors associated with the input features of a linear layer, and let  $\mathbf{c}_{\text{out}} \in [0, 1]^{d_{\text{out}}}$  and  $\mathbf{m}_{\text{out}} \in [0, 1]^{d_{\text{out}}}$  denote the corresponding quantities for the output neurons. We define the observedness vector as  $\mathbf{o}_{\text{in}} = 1 - \mathbf{m}_{\text{in}}$ . All channel vectors are treated as row vectors.

Consider a linear transformation with weight matrix  $W \in \mathbb{R}^{d_{\text{out}} \times d_{\text{in}}}$ . ChannelProp constructs a non-negative routing matrix

$$A = |W| + \epsilon,$$

where  $|\cdot|$  denotes elementwise absolute value and  $\epsilon$  is a small constant for numerical stability. Row-normalization yields

$$\tilde{A}_{ij} = \frac{A_{ij}}{\sum_k A_{ik}}.$$

Confidence and observedness are propagated as weighted mixtures:

$$\mathbf{c}_{\text{out}} = \mathbf{c}_{\text{in}} \tilde{A}^T, \quad \mathbf{o}_{\text{out}} = \mathbf{o}_{\text{in}} \tilde{A}^T,$$

and the output missingness channel is defined as

$$\mathbf{m}_{\text{out}} = 1 - \mathbf{o}_{\text{out}}.$$

All propagated signals are clipped to  $[0, 1]$ .

ChannelProp introduces deterministic parameters and depends solely on the linear weights. While missingness is binary at the input layer, the propagated channel becomes a soft reliability signal reflecting partial dependence on missing inputs. This allows evolved activations to modulate their behavior continuously based on propagated reliability information.

### 3.4 Fitness evaluation

The fitness of a candidate activation tree  $T$  is assessed by embedding it into a three-channel MLP (3C-MLP) and evaluating its predictive performance under a constrained training period. This short horizon evaluation enables efficient exploration of the activation search space while preserving a meaningful correlation between fitness and generalization performance.

**3.4.1 Evaluation protocol.** For each candidate activation, we construct a 3C-MLP in which all hidden layers use the same evolved activation  $T$ . The network is trained on the training split using the Adam optimizer with a fixed learning rate and weight decay, and early stopping is applied with a small patience to limit overfitting and computational cost. Validation accuracy has been tracked during training, and the best validation accuracy  $A_{\text{val}}(T)$  detected during this process is stored.

**3.4.2 Fitness function.** The overall fitness of a tree  $T$  is defined as

$$F(T) = A_{\text{val}}(T) + \lambda_d D(T) - \lambda_s N(T) - \lambda_h (H(T) - 1), \quad (2)$$

where  $D(T) \in \{0, 1, 2, 3\}$  counts the number of distinct input channels  $(\tilde{x}, m, c)$  referenced by the tree,  $N(T)$  is the number of nodes, and  $H(T)$  is the tree depth. Trees of depth  $H = 1$  are assigned zero fitness to eliminate trivial identity-like activations.

The coefficient  $\lambda_d$  provides a mild incentive for utilizing reliability metadata, while  $\lambda_s$  and  $\lambda_h$  penalize excessive size and depth to control code bloat. In all experiments, these coefficients are fixed to  $(\lambda_d, \lambda_s, \lambda_h) = (0.01, 0.0001, 0.0002)$ .

This fitness function achieves a balance between the accuracy of predictions, the simplicity of the structure, and the use of the channels. The diversity term makes sure that the evolved functions use the information about missingness and confidence, preventing degenerate solutions that reduce to simple single-input activations. The complexity components make sure that the evolved expressions are simple to understand and work well outside of the limited prediction window employed during evolution.

### 3.5 GP Representation and Search

Each candidate activation function is represented as a symbolic expression tree defining a multivariate nonlinearity  $f(\tilde{x}, m, c)$ , where  $\tilde{x}$  denotes the imputed feature value,  $m$  the missingness indicator, and  $c$  the propagated confidence score. This representation allows evolved activations to condition explicitly on reliability metadata.

**3.5.1 Terminal and function sets.** The terminal set consists of the three input channels  $\{\tilde{x}, m, c\}$  and a fixed set of real-valued constants  $C = \{0, \pm 0.1, \pm 0.5, \pm 1, \pm 2\}$ . The function set includes unary operators (e.g., tanh, logistic sigmoid aka  $\sigma$ , ReLU, softplus, exp,  $\log|\cdot|$ , square, absolute value) and binary operators (addition, subtraction, multiplication, protected division with a small  $\epsilon$  added when  $|x_2|$  is close to zero, min, and max). All operators are applied elementwise with numerical safeguards to ensure stability. Complete operator lists are provided in Tables 1 and 2.

**Table 1: Unary operators available to the GP search.**

UNARY OPERATIONS			
$x$	$-x$	$ x $	$x^2$
$x^3$	$\sqrt{x}$	$\exp(x)$	$\log( x )$
$\sin(x)$	$\cos(x)$	$\tanh(x)$	$\sigma(x)$
$\text{ReLU}(x)$	$\text{LeakyReLU}(x)$	$\text{ELU}(x)$	$\text{softplus}(x)$

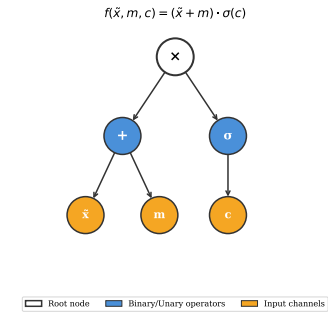


**Figure 1: Tree representation of an evolved three-channel activation function.**

**Table 2: Binary operators available to the GP search.**

BINARY OPERATIONS		
$x_1 + x_2$	$x_1 - x_2$	$x_1 \cdot x_2$
$x_1/x_2$	$\max(x_1, x_2)$	$\min(x_1, x_2)$

**3.5.2 Evolutionary search.** Activation trees are evolved using a generational GP algorithm with fitness-proportional selection, subtree crossover, and mutation. To control excessive growth and maintain interpretability, trees are constrained to a maximum depth throughout initialization and variation, and elitism preserves the top-performing individuals across generations. The algorithm is found in Algorithm 1. Evolutionary hyperparameters are fixed across all experiments and summarized in Table 3.

## 4 Experiments, Results, and Discussion

We present, in turn, our experimental setup, results on datasets with inherently missing data, results on datasets that are inherently complete but from which we synthetically remove data to rigorously study various kinds of missing data, results on an ablation study to demonstrate the contribution of each component of our proposed system, and an analysis of the evolved activation functions.

**Algorithm 1** Evolution of three-channel activation functions (3C-EA)

**Require:** Dataset  $\mathcal{D}$  with missing values, GP parameters  
**Ensure:** Best evolved activation  $T^*$

- 1: Construct three-channel inputs  $(\tilde{x}, m, c)$  using mean imputation, missingness masks, and feature-wise confidence
- 2: Initialize population  $\mathcal{P}_0$  of activation trees with bounded depth
- 3: **for**  $g = 1$  to  $G$  **do**
- 4:     **for all**  $T \in \mathcal{P}_{g-1}$  **do**
- 5:         Embed  $T$  into a three-channel MLP
- 6:         Train network under short horizon with early stopping
- 7:         Evaluate fitness  $F(T)$  using validation accuracy and complexity penalties
- 8:     **end for**
- 9:     Select parents via softmax fitness-proportional sampling
- 10:    Generate offspring via subtree crossover and mutation
- 11:    Preserve top  $k$  individuals by elitism
- 12:    Form next population  $\mathcal{P}_g$
- 13: **end for**
- 14: **return**  $T^* = \arg \max_{T \in \bigcup_{g=0}^G \mathcal{P}_g} F(T)$

**Table 3: GP hyperparameters.**

Parameter	Value
Population size	100
Generations	30
Maximum tree depth	3
Crossover probability	0.7
Mutation probability	0.15
Elite size	2

## 4.1 Experimental Setup

**4.1.1 Datasets.** We evaluate our method using two different types of datasets from the UCI Machine Learning Repository [2]. Dataset details and information about missing data are presented in Table 4. This experimental design provides the evaluation of model performance under both naturally existing and intentionally generated missing data scenarios. The first category includes datasets that already have missing values, mirroring real-world data collecting methods where incompleteness happens naturally rather than through simulation. The datasets include Hepatitis, HouseVotes84, Credit Approval, Mammographic Masses, Cylinder Bands, Heart Disease, and Adult. The datasets reflect significant variation in size, feature dimensionality, feature type, and the level of missing data, with the proportion of incomplete instances varying from moderate to severe. This diversity offers a practical framework to evaluate durability in the presence of naturally partial data.

The second group includes datasets that are naturally complete and free of missing parameters, including Mushroom, WDBC, Pima, Sonar, and Glass. In these datasets, missingness is intentionally generated in a controlled manner to help with systematic study under standardized conditions. The following section goes into more detail on the missingness mechanisms and the injection methods.

**4.1.2 Preprocessing.** For all datasets, missing values are imputed using mean imputation generated entirely from the training data. A

**Table 4: Datasets used in the experiments.**

Name	Inst.	Features	Feature Type	Classes	Incomplete (%)
Hepatitis	155	19	Mixed	2	48.39
HouseVotes84	435	16	Cat	2	46.67
Credit Approval	690	14	Mixed	2	4.20
MammographicMass	961	5	Mixed	2	13.53
Cylinder Bands	512	39	Mixed	2	38.0
Heart Disease	303	13	Mixed	2	6.6
Adult	48842	14	Mixed	2	7.4
HorseColic	368	27	Mixed	3	63.0
Mushroom	8124	22	Cat	2	0
WDBC	569	30	Num	2	0
Pima	768	8	Num	2	0
Sonar	208	60	Num	2	0
Glass	214	9	Num	6	0

binary signal indicating missingness is generated to show whether each feature was initially observed or missing together with the values of the imputed feature. An imputation-confidence score is computed for each feature entry, starting at 1 for observed features and decreasing for imputed entries according to the missingness frequency derived from the training data. This enables the proposed technique to differentiate between the observed and imputed features.

**4.1.3 Evaluation Metrics and Experimental Protocol.** We use Accuracy, Precision, Recall (Sensitivity), Specificity, F1-score, and Area Under the ROC Curve (AUC) as the metrics to evaluate the performance of the classification task [10, 19]. In order to make our results robust and reproducible, all experiments are performed with 30 different runs and random seeds. For each metric, we calculate the mean and standard deviation.

**4.1.4 Baselines and Implementation.** We evaluate 3C-EA against standard fixed activation functions including ReLU, Swish, Leaky ReLU, and ELU. Baseline models use neural network architectures, optimization strategy, preprocessing pipeline, and data partitions identical to the proposed method, differing only in the selection of the activation function. This guarantees that performance divergence is entirely related to the activation design, without influence from other factors. The proposed Three-Channel Evolved Activations (3C-EA) have been evaluated using a three-channel multilayer perceptron (3C-MLP) architecture, in which each nonlinear layer employs a unique evolved activation function  $f(x, m, c)$ . Activation functions are specially constructed for each dataset by GP, as detailed in Table 3.

## 4.2 Results on Real World Incomplete Datasets

We start our empirical examination on datasets that naturally contain missing values, matching real-world techniques for collecting data where incompleteness occurs naturally rather than through controlled simulation. For these datasets, no artificial missingness is introduced. The models function directly on the original incomplete data distributions. All datasets are divided into training, validation, and test sets utilizing fixed splits that are uniformly applied across all methods to guarantee fair comparison. Table 5 summarizes the statistical results for all real world incomplete datasets. Performance is assessed by six standard metrics: accuracy, precision, sensitivity (recall), specificity, F1-score, and area under the ROC curve (AUC).

**Table 5: Performance Comparison on Real World Incomplete datasets.**

Dataset	Method	TestAcc	Prec	Rec	Spec	F1	AUC
Hepatitis	3C-EA	<b>0.8039±0.0407</b>	0.8478±0.0748	0.9283±0.0846	0.3771±0.3449	<b>0.8796±0.0263</b>	0.7195±0.2005
	ReLU	0.7703±0.0550	0.8048±0.0373	0.9333±0.0850	0.2114±0.3449	0.8614±0.0419	0.6183±0.1908
	Swish	0.7535±0.1234	0.8690±0.1899	0.7767±0.2051	0.6743±0.3449	0.8096±0.1741	<b>0.8374±0.0936</b>
	LeakyReLU	0.7935±0.0428	0.8250±0.0540	<b>0.9400±0.0528</b>	0.2914±0.2664	0.8761±0.0238	0.6931±0.2170
	ELU	0.7913±0.0610	<b>0.9128±0.0567</b>	0.8267±0.0620	<b>0.7143±0.2138</b>	0.8652±0.0423	0.8214±0.0947
HouseVotes	3C-EA	<b>0.9407±0.0191</b>	<b>0.9027±0.0469</b>	0.9503±0.0476	<b>0.9348±0.0352</b>	<b>0.9241±0.0240</b>	<b>0.9858±0.0088</b>
	ReLU	0.9126±0.0220	0.8654±0.0506	0.9188±0.0684	0.9089±0.0352	0.8882±0.0287	0.9768±0.0120
	Swish	0.9053±0.0226	0.8485±0.0492	0.9212±0.0653	0.8956±0.0352	0.8805±0.0277	0.9732±0.0129
	LeakyReLU	0.9034±0.0163	0.8510±0.0289	0.9067±0.0599	0.9015±0.0260	0.8762±0.0240	0.9744±0.0117
	ELU	0.9255±0.0276	0.8631±0.0550	<b>0.9612±0.0398</b>	0.9037±0.0448	0.9080±0.0323	0.9792±0.0138
Credit Approval	3C-EA	<b>0.8455±0.0191</b>	<b>0.8096±0.0321</b>	0.8536 ± 0.0254	<b>0.8420±0.0363</b>	<b>0.8366±0.0180</b>	<b>0.9092±0.0158</b>
	ReLU	0.8367 ± 0.0226	0.8086 ± 0.0492	0.8339 ± 0.0437	0.8390 ± 0.0363	0.8189 ± 0.0210	0.9027 ± 0.0143
	Swish	0.8304 ± 0.0249	0.8067 ± 0.0544	0.8208 ± 0.0446	0.8381 ± 0.0363	0.8110 ± 0.0212	0.8960 ± 0.0136
	LeakyReLU	0.8319 ± 0.0251	0.7997 ± 0.0417	0.8317 ± 0.0293	0.8320 ± 0.0500	0.8143 ± 0.0230	0.9021 ± 0.0144
	ELU	0.8425 ± 0.0217	0.7985 ± 0.0312	<b>0.8628±0.0241</b>	0.8264 ± 0.0329	0.8290 ± 0.0218	0.9043 ± 0.0168
Memographic	3C-EA	<b>0.8118 ± 0.0159</b>	<b>0.7798 ± 0.0233</b>	<b>0.8510 ± 0.0285</b>	<b>0.7753 ± 0.0323</b>	<b>0.8133 ± 0.0157</b>	<b>0.8854 ± 0.0084</b>
	ReLU	0.7971 ± 0.0135	0.7652 ± 0.0286	0.8400 ± 0.0469	0.7572 ± 0.0323	0.7793 ± 0.0150	0.8789 ± 0.0119
	Swish	0.7940 ± 0.0131	0.7637 ± 0.0210	0.8315 ± 0.0399	0.7591 ± 0.0323	0.7952 ± 0.0149	0.8706 ± 0.0126
	LeakyReLU	0.8036 ± 0.0152	0.7740 ± 0.0345	0.8430 ± 0.0478	0.7670 ± 0.0553	0.8051 ± 0.0149	0.8802 ± 0.0100
	ELU	0.7945 ± 0.0113	0.7562 ± 0.0220	0.8490 ± 0.0335	0.7437 ± 0.0355	0.7791 ± 0.0116	0.8606 ± 0.0115
Cylinderbands	3C-EA	0.6541 ± 0.0240	0.6812 ± 0.0186	0.7148 ± 0.0458	0.5487 ± 0.0418	0.6969 ± 0.0255	0.6940 ± 0.0242
	ReLU	0.6348 ± 0.0477	0.6294 ± 0.0424	<b>0.9129±0.0830</b>	0.2600 ± 0.0418	<b>0.7414±0.0294</b>	0.6433 ± 0.0967
	Swish	0.6478 ± 0.0345	0.6571 ± 0.0376	0.8316 ± 0.1035	0.4000 ± 0.0418	0.7290 ± 0.0291	0.6622 ± 0.0718
	LeakyReLU	0.6415 ± 0.0435	0.6433 ± 0.0378	0.8632 ± 0.1008	0.3426 ± 0.1638	0.7329 ± 0.0373	0.6593 ± 0.0677
	ELU	<b>0.6637 ± 0.0308</b>	<b>0.9212±0.0245</b>	0.7465 ± 0.0404	<b>0.5522 ± 0.0426</b>	0.7179 ± 0.0283	<b>0.7130 ± 0.0271</b>
Heart Disease	3C-EA	<b>0.9198 ± 0.0482</b>	<b>0.9218 ± 0.0587</b>	<b>0.9242 ± 0.0374</b>	<b>0.9152 ± 0.0681</b>	<b>0.9225 ± 0.0451</b>	<b>0.9636 ± 0.0294</b>
	ReLU	0.8246 ± 0.0164	0.8246 ± 0.0390	0.8415 ± 0.0622	0.8068 ± 0.0681	0.8302 ± 0.0207	0.9112 ± 0.0103
	Swish	0.8041 ± 0.0615	0.7930 ± 0.0633	0.8560 ± 0.0514	0.7496 ± 0.0681	0.8196 ± 0.0331	0.8853 ± 0.1206
	LeakyReLU	0.8281 ± 0.0203	0.8216 ± 0.0308	0.8518 ± 0.0486	0.8032 ± 0.0465	0.8350 ± 0.0217	0.9167 ± 0.0116
	ELU	0.8353 ± 0.0184	0.8192 ± 0.0244	0.8720 ± 0.0294	0.7968 ± 0.0346	0.8443 ± 0.0176	0.9245 ± 0.0219
Adult	3C-EA	<b>0.8241 ± 0.0055</b>	<b>0.6662 ± 0.0094</b>	<b>0.5408 ± 0.0314</b>	0.9141 ± 0.0047	<b>0.5966 ± 0.0221</b>	<b>0.8682 ± 0.0070</b>
	ReLU	0.7596 ± 0.0023	0.2445 ± 0.2682	0.0101 ± 0.0213	<b>0.9975 ± 0.0047</b>	0.0185 ± 0.0383	0.5664 ± 0.0598
	Swish	0.7922 ± 0.0073	0.6326 ± 0.1289	0.3080 ± 0.0835	0.9458 ± 0.0047	0.4077 ± 0.0966	0.7990 ± 0.0383
	LeakyReLU	0.7654 ± 0.0132	0.3671 ± 0.3678	0.0543 ± 0.1159	0.9911 ± 0.0198	0.0764 ± 0.1483	0.6150 ± 0.0994
	ELU	0.7990 ± 0.0096	0.6589 ± 0.0180	0.3434 ± 0.0697	0.9436 ± 0.0111	0.4476 ± 0.0587	0.8183 ± 0.0287

The experiments show a clear advantage for 3C-EA, which achieves the highest test accuracy on six out of seven datasets (Table 5). On Heart Disease, 3C-EA has the best test accuracy (0.9198) and F1-score (0.9225), which is a 9 percentage point improvement over ReLU. On Adult, 3C-EA achieves the best accuracy (0.8241) and significantly boosts the recall (0.5408) compared to ReLU (0.0101), showing a better capability of handling the minority class in imbalanced problems. On HouseVotes84 and Credit Approval, 3C-EA clearly outperforms baselines across all metrics, with HouseVotes84 achieving accuracy 0.9407 and AUC 0.9858. On Cylinder Bands, where the baseline methods are challenged by 38% missing data, 3C-EA shows a large improvement in specificity (0.5487 vs. 0.2600 of ReLU), showing a better performance in the presence of poor-quality data. The Adult dataset serves as a severe stress test because it contains many samples (48,842), is naturally incomplete, and is extremely imbalanced. In this scenario, 3C-EA has the best overall accuracy (0.8241) and an even higher recall rate (0.5408), proving that it is not just predicting the majority class. This supports the primary claim that modifying activations on value, missingness, and confidence enables the network to more effectively manage real-world incomplete tabular data by differentiating between observed and imputed inputs.

### 4.3 Results on Complete Datasets

We evaluate our method (3C-EA) against missingness by adding 20% missingness to originally complete datasets using the MNAR, MCAR, and MAR methods. In order to prevent degenerate sparsity, this fixed rate allows for direct comparison among techniques. All

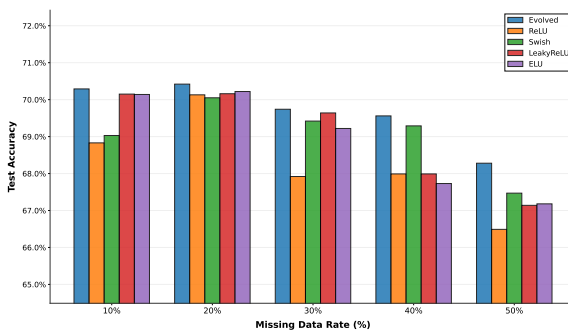
approaches use the same preprocessing, divisions, architectures, and training protocols.

**4.3.1 MNAR Missingness.** MNAR is the most difficult case, in which the missingness is related to the values themselves. The results are shown in Table 6. In the six-class imbalanced, Glass dataset, 3C-EA shows an accuracy of 52.5%, surpassing the baseline range of 40.7% to 49.8% (an improvement of 2.7% to 11.8%). The F1-score rises to 0.338 from a range of 0.210–0.331, while the AUC improves to 0.773 from a range of 0.648–0.730. The reason for this is ChannelProp: in MNAR, extreme values are more vulnerable to being missing, and the evolved functions of 3C-EA explicitly condition on distributed confidence scores to modify responses accordingly. On the Pima dataset, in addition to that, our method shows the highest values on accuracy; it also has the highest recall of 0.412, surpassing ReLU (0.260), Swish (0.376), and LeakyReLU (0.319), while ELU is roughly comparable at 0.411. Regarding the F1-score, 3C-EA (0.486) surpassed ReLU, Swish, and LeakyReLU, however ELU had somewhat superior performance (0.494). The increase in recall demonstrates that reliability aware activations prevent majority class collapse in uncertain conditions. Also, 3C-EA displays the best accuracy (93.1%) and F1-score (0.905), which shows that it works well on the WDBC which is a clinical breast cancer dataset. In Sonar with 60 features, 3C-EA has the highest accuracy (76.1%), F1-score (0.779), and AUC (0.840) among the methods, showing that ChannelProp effectively scales in high-dimensional datasets. Additionally, in the Mushroom dataset with 8,124 samples, it has the highest accuracy of 98.5% with the lowest variance of ±0.097 when compared to baselines of ±0.019–0.028, indicating stable large-scale optimization.

**Table 6: MNAR Imputed datasets results.**

Dataset	Method	TestAcc	Prec	Rec	Spec	F1	AUC
Sonar	3C-EA	<b>0.7619±0.0447</b>	<b>0.7591±0.0536</b>	<b>0.8106±0.0722</b>	0.7160±0.0674	<b>0.7791±0.0423</b>	<b>0.8395±0.0304</b>
	ReLU	0.7467±0.0499	0.7382±0.0448	0.8073±0.1215	0.6800±0.0674	0.7655±0.0616	0.8190±0.0481
	Swish	0.7400±0.0495	0.7546±0.0504	0.7618±0.1422	0.7160±0.0674	0.7479±0.0724	0.8214±0.0360
	LeakyReLU	0.7393±0.0352	0.7567±0.0453	0.8055±0.0905	0.7080±0.0868	0.7761±0.0410	0.8368±0.0395
	ELU	0.7362±0.0409	0.7586±0.0670	0.7418±0.0526	<b>0.7300±0.0990</b>	0.7469±0.0335	0.7994±0.0422
Glass	3C-EA	<b>0.5247±0.0784</b>	<b>0.3381±0.0972</b>	<b>0.3773±0.0812</b>	0.8874±0.0181	<b>0.3390±0.0868</b>	<b>0.7729±0.0745</b>
	ReLU	0.4065±0.1059	0.2093±0.0938	0.2839±0.0681	0.8874±0.0181	0.2124±0.0759	0.6475±0.0832
	Swish	0.4400±0.0627	0.2535±0.0829	0.3152±0.0383	0.8874±0.0181	0.2540±0.0531	0.7300±0.0603
	LeakyReLU	0.4521±0.0535	0.2233±0.1057	0.2935±0.0621	0.8874±0.0181	0.2361±0.0796	0.6486±0.0872
	ELU	0.4977±0.0724	0.3313±0.0933	0.3537±0.0645	0.8874±0.0181	0.3112±0.0680	0.7025±0.0752
WDBC	3C-EA	<b>0.9312±0.0273</b>	<b>0.9281±0.0428</b>	<b>0.8914±0.0621</b>	<b>0.9591±0.0721</b>	<b>0.9045±0.0405</b>	0.9733±0.0241
	ReLU	0.9221±0.0205	0.9262±0.0441	0.8610±0.0556	0.9578±0.0265	0.8903±0.0290	<b>0.9835±0.0069</b>
	Swish	0.9196±0.0156	0.8997±0.0503	0.8857±0.0442	0.9394±0.0265	0.8906±0.0194	0.9833±0.0052
	LeakyReLU	0.9232±0.0157	0.9184±0.0414	0.8724±0.0542	0.9528±0.0269	0.8928±0.0239	0.9814±0.0129
	ELU	0.9263±0.0233	0.9142±0.0557	0.8876±0.0372	0.9489±0.0364	0.8992±0.0295	0.9819±0.0129
PIMA	3C-EA	<b>0.7042±0.0209</b>	0.6043±0.0497	<b>0.4121±0.0763</b>	0.8574±0.0350	<b>0.4856±0.0642</b>	<b>0.73061±0.0376</b>
	ReLU	0.6956±0.0276	0.6310±0.1654	0.2604±0.1395	<b>0.9240±0.0350</b>	0.3485±0.1477	0.7073±0.0643
	Swish	0.7005±0.0213	0.6260±0.0718	0.3758±0.1482	0.8709±0.0350	0.4457±0.1148	0.7343±0.0234
	LeakyReLU	0.7016±0.0281	<b>0.6480±0.0757</b>	0.3192±0.1103	0.9022±0.0639	0.4135±0.0965	0.7305±0.0314
	ELU	0.7022±0.0152	0.6294±0.0469	0.4113±0.0562	0.8701±0.0346	0.4940±0.0393	0.7274±0.0189
Mushroom	3C-EA	<b>0.9850 ± 0.0097</b>	<b>0.9831 ± 0.0092</b>	<b>0.9858 ± 0.0118</b>	<b>0.9850 ± 0.0098</b>	<b>0.9844 ± 0.0101</b>	<b>0.9973 ± 0.0038</b>
	ReLU	0.9426 ± 0.0284	0.9637 ± 0.0084	0.9153 ± 0.0580	0.9417 ± 0.0294	0.9380 ± 0.0326	0.9807 ± 0.0174
	Swish	0.9086 ± 0.0192	0.9383 ± 0.0136	0.8674 ± 0.0386	0.9071 ± 0.0198	0.9010 ± 0.0224	0.9557 ± 0.0239
	LeakyReLU	0.9399 ± 0.0276	0.9571 ± 0.0131	0.9162 ± 0.0517	0.9391 ± 0.0284	0.9356 ± 0.0311	0.9797 ± 0.0187
	ELU	0.9666 ± 0.0201	0.9696 ± 0.0143	0.9606 ± 0.0292	0.9664 ± 0.0205	0.9650 ± 0.0217	0.9933 ± 0.0089

**4.3.2 MCAR Missingness.** Results related to MCAR missingness are presented in Table 7. On the Glass dataset, regarding uninformative missingness, 3C-EA achieves the highest accuracy of 53.2%, surpassing the baselines which range from 45.5% to 50.2%. The F1-score improves from 0.242–0.336 to 0.367. This shows that confidence data is useful even when the missingness patterns don't contain any information, GP-evolved activations are able to determine appropriate weights to imputed versus actual values depending on feature-specific reliability. Our method achieves the highest recall (0.469), F1-score (0.523), and AUC (0.744) on PIMA in comparison to the baseline models. The recall has increased significantly compared to the baselines, confirming that the three-channel activation provides a comprehensive strategy to handle uncertainty, rather than only exploiting patterns of missing data. Figure 2 illustrates the effectiveness of our approach on PIMA with missing rates ranging from 10% to 50%. The performance gap between 3C-EA and the baselines grows with the missing rate, showing that the reliability information is more beneficial in conditions of poor data quality.

**Figure 2: Performance comparison across missing data rates (10%-50%) on the PIMA dataset.**

**4.3.3 MAR Missingness.** Table 8 presents results under MAR missingness, when the missingness is conditional upon observable features. In this context, 3C-EA shows its most significant advantages on more difficult datasets. On Glass, 3C-EA demonstrates optimal performance, achieving 58.0% accuracy, in contrast to the baseline range of 45.6–57.9%. While ELU exhibits a little better F1-score (0.374 versus 0.372), 3C-EA demonstrates the highest AUC (0.778) in contrast to the range of 0.665–0.754, indicating enhanced probability calibration across all six classes. The superior performance of MAR is credited to ChannelProp's effective representation of the conditional missingness pattern in the network, permitting evolved activations to learn from the features responsible for the missing values. On PIMA, our method achieves the highest accuracy (70.2%), recall (0.493), F1-score (0.530), and AUC (0.743) compared to all other approaches. The relative recall increases are most significant for ReLU (18.3 points) and LeakyReLU (18.6 points). On WDBC, we achieves the highest accuracy (93.5%), precision (0.918), specificity (0.955), F1-score (0.912), and AUC (0.990), confirming consistent improvements in this medical diagnostic test.

#### 4.4 Ablation Study

To evaluate the contribution of each component in our method, we run ablation experiments on four selected datasets (Glass, Sonar, WDBC, PIMA) under challenging circumstances, including MNAR missingness with a missing rate of 40% and a population size of 50. The reason for choosing such challenging settings is that MNAR is the most difficult type of missing data [26], where the missingness is a function of the unobserved data itself, and the missing rate of 40% is chosen to make the reliability information even more important for prediction. The results in Table 9 reveal that removing of any element causes to a consistent decrease of performance, thus demonstrating the importance of missingness indicators, confidence propagation, and the joint modeling of both in evolved activation functions.

**Table 7: MCAR Imputed datasets results.**

Dataset	Method	TestAcc	Prec	Rec	Spec	F1	AUC
Sonar	3C-EA	0.7413 $\pm$ 0.0626	0.7436 $\pm$ 0.0573	0.7803 $\pm$ 0.1214	0.6983 $\pm$ 0.1099	0.7561 $\pm$ 0.0717	0.8084 $\pm$ 0.0626
	ReLU	0.7437 $\pm$ 0.0635	0.7197 $\pm$ 0.0590	0.8561 $\pm$ 0.1144	0.6200 $\pm$ 0.1099	0.7756 $\pm$ 0.0633	0.8208 $\pm$ 0.0799
	Swish	0.7405 $\pm$ 0.0666	0.7187 $\pm$ 0.0531	0.8379 $\pm$ 0.1310	0.6333 $\pm$ 0.1099	0.7680 $\pm$ 0.0701	0.8205 $\pm$ 0.0505
	LeakyReLU	0.7468 $\pm$ 0.0613	0.7316 $\pm$ 0.0645	0.8409 $\pm$ 0.1455	0.6433 $\pm$ 0.1377	0.7714 $\pm$ 0.0739	0.8300 $\pm$ 0.0397
	ELU	0.7556 $\pm$ 0.0529	0.7625 $\pm$ 0.0593	0.7833 $\pm$ 0.0884	0.7250 $\pm$ 0.0920	0.7691 $\pm$ 0.0550	0.8155 $\pm$ 0.0544
Glass	3C-EA	0.5318 $\pm$ 0.1038	0.3922 $\pm$ 0.1411	0.4023 $\pm$ 0.0939	0.8896 $\pm$ 0.0238	0.3668 $\pm$ 0.1165	0.7677 $\pm$ 0.1037
	ReLU	0.4550 $\pm$ 0.0906	0.2525 $\pm$ 0.1043	0.2994 $\pm$ 0.0689	0.8896 $\pm$ 0.0238	0.2423 $\pm$ 0.0811	0.7068 $\pm$ 0.0782
	Swish	0.4558 $\pm$ 0.0873	0.2554 $\pm$ 0.0964	0.3198 $\pm$ 0.0711	0.8896 $\pm$ 0.0238	0.2534 $\pm$ 0.0813	0.7575 $\pm$ 0.0953
	LeakyReLU	0.4721 $\pm$ 0.0682	0.2998 $\pm$ 0.0969	0.3246 $\pm$ 0.0620	0.8896 $\pm$ 0.0238	0.2758 $\pm$ 0.0682	0.7462 $\pm$ 0.0855
	ELU	0.5023 $\pm$ 0.1043	0.3550 $\pm$ 0.1318	0.3801 $\pm$ 0.1054	0.8896 $\pm$ 0.0238	0.3361 $\pm$ 0.1143	0.7475 $\pm$ 0.0896
WDBC	3C-EA	0.9415 $\pm$ 0.0154	0.9383 $\pm$ 0.0367	0.9032 $\pm$ 0.0464	0.9639 $\pm$ 0.0228	0.9189 $\pm$ 0.0233	0.9832 $\pm$ 0.0102
	ReLU	0.9246 $\pm$ 0.0163	0.9399 $\pm$ 0.0461	0.8532 $\pm$ 0.0435	0.9662 $\pm$ 0.0228	0.8928 $\pm$ 0.0232	0.9821 $\pm$ 0.0079
	Swish	0.9164 $\pm$ 0.0249	0.9029 $\pm$ 0.0684	0.8770 $\pm$ 0.0587	0.9394 $\pm$ 0.0228	0.8859 $\pm$ 0.0300	0.9822 $\pm$ 0.0056
	LeakyReLU	0.9246 $\pm$ 0.0208	0.9478 $\pm$ 0.0546	0.8468 $\pm$ 0.0545	0.9699 $\pm$ 0.0342	0.8919 $\pm$ 0.0303	0.9806 $\pm$ 0.0123
	ELU	0.9316 $\pm$ 0.0195	0.9361 $\pm$ 0.0454	0.8770 $\pm$ 0.0384	0.9634 $\pm$ 0.0286	0.9043 $\pm$ 0.0263	0.9831 $\pm$ 0.0109
PIMA	3C-EA	0.7093 $\pm$ 0.0204	0.6102 $\pm$ 0.0457	0.4687 $\pm$ 0.0449	0.8325 $\pm$ 0.0426	0.5237 $\pm$ 0.0262	0.7437 $\pm$ 0.0194
	ReLU	0.6958 $\pm$ 0.0249	0.6249 $\pm$ 0.1570	0.2823 $\pm$ 0.1254	0.9129 $\pm$ 0.0426	0.3714 $\pm$ 0.1382	0.6919 $\pm$ 0.0543
	Swish	0.7005 $\pm$ 0.0230	0.6285 $\pm$ 0.0924	0.3819 $\pm$ 0.1235	0.8677 $\pm$ 0.0426	0.4552 $\pm$ 0.0929	0.7261 $\pm$ 0.0205
	LeakyReLU	0.7075 $\pm$ 0.0268	0.6547 $\pm$ 0.0679	0.3442 $\pm$ 0.0781	0.8982 $\pm$ 0.0554	0.4425 $\pm$ 0.0700	0.7216 $\pm$ 0.0355
	ELU	0.7034 $\pm$ 0.0323	0.6033 $\pm$ 0.0673	0.4370 $\pm$ 0.0862	0.8432 $\pm$ 0.0611	0.4998 $\pm$ 0.0633	0.7292 $\pm$ 0.0334
Mushroom	3C-EA	0.9850 $\pm$ 0.0097	0.9831 $\pm$ 0.0092	0.9858 $\pm$ 0.0118	0.9850 $\pm$ 0.0098	0.9844 $\pm$ 0.0101	0.9973 $\pm$ 0.0038
	ReLU	0.9426 $\pm$ 0.0284	0.9637 $\pm$ 0.0084	0.9153 $\pm$ 0.0580	0.9417 $\pm$ 0.0294	0.9380 $\pm$ 0.0326	0.9807 $\pm$ 0.0174
	Swish	0.9086 $\pm$ 0.0192	0.9383 $\pm$ 0.0136	0.8674 $\pm$ 0.0386	0.9071 $\pm$ 0.0198	0.9010 $\pm$ 0.0224	0.9557 $\pm$ 0.0239
	LeakyReLU	0.9399 $\pm$ 0.0276	0.9571 $\pm$ 0.0131	0.9162 $\pm$ 0.0517	0.9391 $\pm$ 0.0284	0.9356 $\pm$ 0.0311	0.9797 $\pm$ 0.0187
	ELU	0.9666 $\pm$ 0.0201	0.9696 $\pm$ 0.0143	0.9606 $\pm$ 0.0292	0.9664 $\pm$ 0.0205	0.9650 $\pm$ 0.0217	0.9933 $\pm$ 0.0089

**Table 8: MAR Imputed datasets results.**

Dataset	Method	TestAcc	Prec	Rec	Spec	F1	AUC
Sonar	3C-EA	0.7691 $\pm$ 0.0683	0.7611 $\pm$ 0.0747	0.8030 $\pm$ 0.0956	0.7067 $\pm$ 0.1574	0.7760 $\pm$ 0.0565	0.8368 $\pm$ 0.0592
	ReLU	0.7802 $\pm$ 0.0661	0.7759 $\pm$ 0.0668	0.8273 $\pm$ 0.1304	0.7283 $\pm$ 0.1574	0.7936 $\pm$ 0.0751	0.8467 $\pm$ 0.0445
	Swish	0.7778 $\pm$ 0.0489	0.7724 $\pm$ 0.0491	0.8303 $\pm$ 0.1378	0.7200 $\pm$ 0.1574	0.7913 $\pm$ 0.0655	0.8524 $\pm$ 0.0298
	LeakyReLU	0.7595 $\pm$ 0.0613	0.7556 $\pm$ 0.0754	0.8242 $\pm$ 0.1166	0.6883 $\pm$ 0.1453	0.7803 $\pm$ 0.0587	0.8415 $\pm$ 0.0520
	ELU	0.7706 $\pm$ 0.0578	0.7820 $\pm$ 0.0632	0.7864 $\pm$ 0.0848	0.7533 $\pm$ 0.0912	0.7812 $\pm$ 0.0585	0.8286 $\pm$ 0.0548
Glass	3C-EA	0.5803 $\pm$ 0.1060	0.3880 $\pm$ 0.1415	0.3952 $\pm$ 0.0931	0.8976 $\pm$ 0.0264	0.3721 $\pm$ 0.1118	0.7778 $\pm$ 0.1080
	ReLU	0.4558 $\pm$ 0.1184	0.2655 $\pm$ 0.1061	0.2988 $\pm$ 0.0638	0.8976 $\pm$ 0.0264	0.2495 $\pm$ 0.0836	0.6645 $\pm$ 0.0835
	Swish	0.4736 $\pm$ 0.0912	0.2923 $\pm$ 0.0751	0.3277 $\pm$ 0.0602	0.8976 $\pm$ 0.0264	0.2751 $\pm$ 0.0651	0.7366 $\pm$ 0.0751
	LeakyReLU	0.4837 $\pm$ 0.1018	0.2726 $\pm$ 0.0933	0.3173 $\pm$ 0.0574	0.8976 $\pm$ 0.0264	0.2676 $\pm$ 0.0733	0.7062 $\pm$ 0.0517
	ELU	0.5787 $\pm$ 0.0753	0.3796 $\pm$ 0.1090	0.4081 $\pm$ 0.0559	0.8976 $\pm$ 0.0264	0.3735 $\pm$ 0.0772	0.7542 $\pm$ 0.0574
WDBC	3C-EA	0.9354 $\pm$ 0.0212	0.9176 $\pm$ 0.0381	0.9127 $\pm$ 0.0423	0.9546 $\pm$ 0.0254	0.9123 $\pm$ 0.0288	0.9896 $\pm$ 0.0169
	ReLU	0.9272 $\pm$ 0.0211	0.9153 $\pm$ 0.0426	0.8881 $\pm$ 0.0587	0.9500 $\pm$ 0.0254	0.8994 $\pm$ 0.0302	0.9845 $\pm$ 0.0087
	Swish	0.9278 $\pm$ 0.0226	0.8929 $\pm$ 0.0514	0.9198 $\pm$ 0.0531	0.9324 $\pm$ 0.0254	0.9039 $\pm$ 0.0285	0.9848 $\pm$ 0.0053
	LeakyReLU	0.9287 $\pm$ 0.0185	0.9045 $\pm$ 0.0437	0.9056 $\pm$ 0.0474	0.9421 $\pm$ 0.0317	0.9034 $\pm$ 0.0246	0.9846 $\pm$ 0.0057
	ELU	0.9322 $\pm$ 0.0277	0.8882 $\pm$ 0.0586	0.9405 $\pm$ 0.0397	0.9273 $\pm$ 0.0478	0.9117 $\pm$ 0.0322	0.9796 $\pm$ 0.0170
PIMA	3C-EA	0.7021 $\pm$ 0.0203	0.5833 $\pm$ 0.0419	0.4928 $\pm$ 0.0669	0.8119 $\pm$ 0.0458	0.5304 $\pm$ 0.0395	0.7428 $\pm$ 0.0209
	ReLU	0.6969 $\pm$ 0.0243	0.6283 $\pm$ 0.0718	0.3094 $\pm$ 0.1252	0.9002 $\pm$ 0.0458	0.3964 $\pm$ 0.1240	0.7200 $\pm$ 0.0607
	Swish	0.6909 $\pm$ 0.0200	0.5769 $\pm$ 0.0578	0.4619 $\pm$ 0.1279	0.8111 $\pm$ 0.0458	0.4970 $\pm$ 0.0749	0.7367 $\pm$ 0.0199
	LeakyReLU	0.6930 $\pm$ 0.0238	0.6179 $\pm$ 0.0797	0.3072 $\pm$ 0.1118	0.8954 $\pm$ 0.0519	0.3955 $\pm$ 0.1066	0.7371 $\pm$ 0.0326
	ELU	0.6888 $\pm$ 0.0221	0.5581 $\pm$ 0.0400	0.4808 $\pm$ 0.0742	0.7980 $\pm$ 0.0437	0.5129 $\pm$ 0.0462	0.7294 $\pm$ 0.0348
Mushroom	3C-EA	0.9738 $\pm$ 0.0041	0.9682 $\pm$ 0.0055	0.9777 $\pm$ 0.0049	0.9739 $\pm$ 0.0041	0.9729 $\pm$ 0.0042	0.9955 $\pm$ 0.0013
	ReLU	0.9428 $\pm$ 0.0190	0.9451 $\pm$ 0.0065	0.9358 $\pm$ 0.0418	0.9426 $\pm$ 0.0198	0.9399 $\pm$ 0.0221	0.9842 $\pm$ 0.0153
	Swish	0.9009 $\pm$ 0.0161	0.9191 $\pm$ 0.0116	0.8712 $\pm$ 0.0324	0.8999 $\pm$ 0.0166	0.8942 $\pm$ 0.0187	0.9563 $\pm$ 0.0185
	LeakyReLU	0.9244 $\pm$ 0.0211	0.9292 $\pm$ 0.0123	0.9125 $\pm$ 0.0389	0.9240 $\pm$ 0.0217	0.9204 $\pm$ 0.0236	0.9748 $\pm$ 0.0159
	ELU	0.9609 $\pm$ 0.0078	0.9564 $\pm$ 0.0088	0.9628 $\pm$ 0.0094	0.9610 $\pm$ 0.0078	0.9596 $\pm$ 0.0081	0.9932 $\pm$ 0.0027

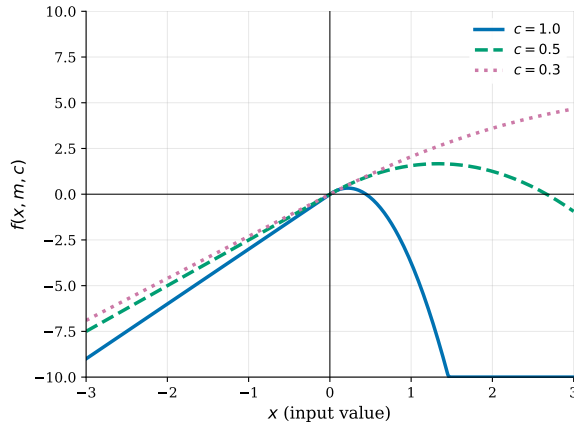
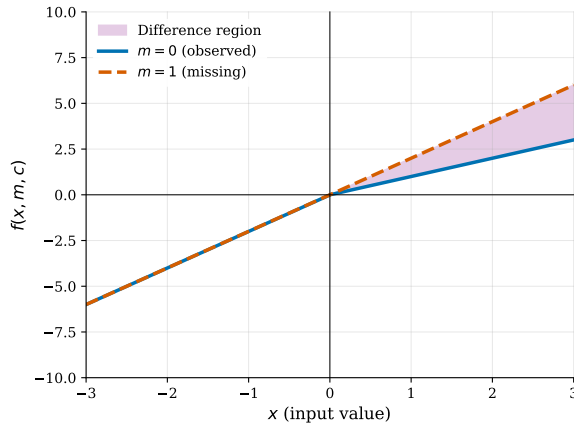
## 4.5 Evolved Activation Function Analysis

To understand the behavior of the evolved activation functions, we analyze solutions found by the GP search and their behavior. Figure 3 presents an evolved activation function demonstrating three-channel awareness. The figure shows the confidence effect: the activation shape transforms from complex nonlinear response at high confidence ( $c = 1.0$ ) to conservative near-linear behavior at low confidence ( $c = 0.3$ ), while holding  $m = 0$ . The evolved function  $f(x, m, c) = x(c+2) \left[ \frac{c}{\text{ReLU}(\max(c, -0.5) - m)} - c \text{ReLU}(1.5cx)(0.5 + c) \right]$  integrates both missing indicators and confidence scores, enabling adaptive behavior based on data reliability. Figure 4 shows a strong activation function that shows its awareness of the missing data. The function  $f(x, m, c) = \min(x \cdot m, x) + x$  shows its conditional behavior based on the missing flag. For positive inputs, when the data

is observed ( $m = 0$ ), the output is  $x$ , but when the data is imputed ( $m = 1$ ), the output is  $2x$ . This shows that the evolutionary process has identified a strong adaptation technique, where the function has gained the capability to enhance the imputed data without any specific design. This suggests that the evolutionary process has created a strong adaptation mechanism, where the function has learned to double the imputed data, possibly to counter the uncertainty of the imputed data. Table 10 shows the winner activation formulae that were developed over 30 independent GP runs on the Hepatitis dataset. The variety of solutions found shows how flexible the three-channel search space is. The fact that missingness and confidence channels are used consistently between runs shows that the suggested method works.

**Table 9: Ablation Study Results.**

Dataset	Variant	TestAcc	F1	AUC
Glass	Full $f(x, m, c)$	$0.435 \pm 0.116$	$0.229 \pm 0.072$	$0.641 \pm 0.233$
	No Conf. $f(x, m)$	$0.407 \pm 0.059$	$0.223 \pm 0.075$	$0.626 \pm 0.085$
	No Flag $f(x, c)$	$0.386 \pm 0.085$	$0.220 \pm 0.063$	$0.631 \pm 0.050$
	No ChannelProp	$0.381 \pm 0.054$	$0.200 \pm 0.066$	$0.611 \pm 0.069$
Sonar	Full $f(x, m, c)$	$0.724 \pm 0.043$	$0.733 \pm 0.061$	$0.786 \pm 0.036$
	No Conf. $f(x, m)$	$0.712 \pm 0.048$	$0.721 \pm 0.071$	$0.780 \pm 0.054$
	No Flag $f(x, c)$	$0.650 \pm 0.088$	$0.632 \pm 0.222$	$0.721 \pm 0.080$
	No ChannelProp	$0.686 \pm 0.089$	$0.700 \pm 0.073$	$0.796 \pm 0.036$
WDBC	Full $(x, m, c)$	$0.9225 \pm 0.0261$	$0.8866 \pm 0.0527$	$0.9693 \pm 0.0160$
	No Conf. $(x, m)$	$0.9149 \pm 0.0215$	$0.8828 \pm 0.0346$	$0.9612 \pm 0.0155$
	No Flag $(x, c)$	$0.9161 \pm 0.0346$	$0.8963 \pm 0.0417$	$0.9768 \pm 0.0146$
	No ChannelProp	$0.9123 \pm 0.0299$	$0.8814 \pm 0.0440$	$0.9718 \pm 0.0135$
PIMA	Full $(x, m, c)$	$0.6922 \pm 0.0301$	$0.4637 \pm 0.1090$	$0.7174 \pm 0.0311$
	No Conf. $(x, m)$	$0.6782 \pm 0.0352$	$0.3980 \pm 0.0980$	$0.7005 \pm 0.0536$
	No Flag $(x, c)$	$0.6741 \pm 0.0211$	$0.4338 \pm 0.0913$	$0.7060 \pm 0.0455$
	No ChannelProp	$0.6701 \pm 0.0258$	$0.4099 \pm 0.1422$	$0.7074 \pm 0.0340$

**Figure 3: Evolved activation function on heart disease dataset demonstrating three-channel confidence effect.****Figure 4: Evolved missing-aware activation functions (Glass dataset).**

## 5 Conclusions and Future Work

This paper proposed Three-Channel Evolved Activations (3C-EA), a GP method for evolving multivariate activation functions  $f(x, m, c)$  that directly includes feature values, missingness indicators, and

**Table 10: Winner Activation Functions Evolved Across 30 Independent GP Runs on the Hepatitis Dataset.**

Run	Acc.	F1	Evolved Formula $f(x, m, c)$
1	0.7742	0.8727	$x^2 \cdot c$
2	0.8387	0.9057	$\min\left(\text{softplus}(x) + \frac{x-2c}{\text{softplus}(m/0.1)}, x\right)$
3	0.8387	0.9020	$\tanh(\max(\min(\exp(\max(m, x)), -0.1),  x )) + x$
4	0.7419	0.8462	$\max(-1, \max(x, \sin x) \cdot \min(x, \frac{x}{\sin x}))$
5	0.8065	0.8571	$x \cdot \max(c, \text{softplus}(-0.1))$
6	0.8065	0.8750	$\frac{x}{0.5} - \max(m, c)$
7	0.7742	0.8444	$(c - m - x) + \cos(x + m + c + 0.5 + \min(c, 2 - c)) - x$
8	0.9032	0.9388	$\text{ELU}(\exp(m + x))$
9	0.9032	0.9362	$0.5 \sin(x)$
10	0.8065	0.8750	$x + \min(x, m - x^2)$
11	0.8387	0.8936	$\sin(\min(x, 0)) + \max(c, \exp(x) - \exp(c + \text{ELU}(\tanh(\exp x))) + x) + 2x$
12	0.6774	0.8000	$\text{ELU}(\text{ReLU}(1 - \frac{x}{c} + m - \text{ReLU}(x) - m + x^3))^2$
13	0.8065	0.8750	$x \cdot (\min(x, x + c + \text{LeakyReLU}(x)) - 1)$
14	0.8065	0.8750	$-\min(x, \min(c^2, m))$
15	0.8065	0.8750	$(c - \max(\cos(2c), x)) \cdot x$
16	0.7419	0.8400	$\sin(x)$
17	0.7742	0.8727	$\min(x, c)$
18	0.8065	0.8800	$c \cdot (m - \min(-\max(x + m \cdot x + \text{ReLU}(x + c)), 0.5))$
19	0.6774	0.7500	$\frac{x}{c}$
20	0.7742	0.8627	$\max(x^2, m)$
21	0.7097	0.8302	$\max(\exp m, \max(c, c^2)) + \frac{0.5 + \cos x}{x} \cdot (x \cdot (c - m))$
22	0.7742	0.8627	$x \cdot (x - (x - c)m) - x$
23	0.7419	0.8462	$x + m$
24	0.8387	0.8837	$\frac{\sqrt{ c } + m - \sqrt{c} + 0.1}{ c } - \sqrt{c} - 2x$
25	0.8710	0.9167	$\min(m, x) - m \cdot (m - (x + \max(x - x, \sqrt{x}\sigma(c))) - x)$
26	0.8387	0.8980	$\frac{\max(x^2 + x, x)}{\tanh(0.1 / \min(\max(-\text{ELU}(\exp(\cos(2)x)), x), m))}$
27	0.8065	0.8750	$x + x^2$
28	0.7419	0.8462	$\max(\min(m, c), x)$
29	0.7097	0.8302	$x - \max(x - m, -\min(x, 2))$
30	0.8387	0.9057	$x - \max(x - m, -\min(x, 2))$

confidence scores. To effectively transmit missingness and confidence information through deep models, we proposed ChannelProp, a deterministic method for propagating missingness and confidence information through linear layers. Experiments on natural and introduced missing data (MCAR, MAR, MNAR) showed that 3C-EA is competitive or even better than standard fixed activation functions (ReLU, Swish, LeakyReLU, ELU). Experiments showed that improvements were consistent across different types of missingness, with significant improvements seen in datasets with higher missing rates and multi-class classification tasks. The study of evolved functions proved that GP can detect effective adaptive strategies, such as enhancing imputed values or modifying activation functions based on confidence levels. Future work includes extending 3C-EA to recurrent and attention-based designs, transferring evolved activations across different domains, and combining heuristic confidence scores with learned estimates.

## References

- [1] Andrea Apicella, Francesco Donnarumma, Francesco Isgò, and Roberto Prevete. 2021. A Survey on Modern Trainable Activation Functions. *Neural Networks* 138 (2021), 14–32.
- [2] Arthur Asuncion and David Newman. 2007. UCI machine learning repository.
- [3] Ibrahim Berkan Aydilek and Ahmet Arslan. 2013. A Hybrid Method for Imputation of Missing Values using Optimized Fuzzy C-Means with Support Vector Regression and a Genetic Algorithm. *Information Sciences* 233 (2013), 25–35.

[4] Gustavo EAPA Batista and Maria Carolina Monard. 2003. An Analysis of Four Missing Data Treatment Methods for Supervised Learning. *Applied Artificial Intelligence* 17, 5-6 (2003), 519–533.

[5] Garrett Bingham, William Macke, and Risto Miikkulainen. 2020. Evolutionary Optimization of Deep Learning Activation Functions. In *Proceedings of the 2020 Genetic and Evolutionary Computation Conference* (Cancún, Mexico) (GECCO '20). Association for Computing Machinery, New York, NY, USA, 289–296. doi:10.1145/3377930.3389841

[6] Zhengping Che, Sanjay Purushotham, Kyunghyun Cho, David Sontag, and Yan Liu. 2018. Recurrent Neural Networks for Multivariate Time Series with Missing Values. *Scientific Reports* 8, 1 (2018), 6085.

[7] Shiv Ram Dubey, Satish Kumar Singh, and Bidyut Baran Chaudhuri. 2022. Activation Functions in Deep Learning: A Comprehensive Survey and Benchmark. *Neurocomputing* 503 (2022), 92–108.

[8] Tlamelo Emmanuel, Thabiso Maupong, Dimane Mpoele, Thabo Semong, Banyatsang Mphago, and Oteng Tabona. 2021. A Survey on Missing Data in Machine Learning. *Journal of Big Data* 8, 1 (2021), 140.

[9] Xavier Glorot and Yoshua Bengio. 2010. Understanding the Difficulty of Training Deep Feedforward Neural Networks. In *Proceedings of the Thirteenth International Conference on Artificial Intelligence and Statistics (Proceedings of Machine Learning Research, Vol. 9)*. JMLR Workshop and Conference Proceedings, PMLR, Chia Laguna Resort, Sardinia, Italy, 249–256.

[10] David J. Hand and Robert J. Till. 2001. A Simple Generalisation of the Area Under the ROC Curve for Multiple Class Classification Problems. *Machine Learning* 45, 2 (2001), 171–186.

[11] José M Jerez, Ignacio Molina, Pedro J García-Laencina, Emilio Alba, Nuria Ribelles, Miguel Martín, and Leonardo Franco. 2010. Missing Data Imputation using Statistical and Machine Learning Methods in a Real Breast Cancer Problem. *Artificial Intelligence in Medicine* 50, 2 (2010), 105–115.

[12] John R Koza. 1994. Genetic Programming as a Means for Programming Computers by Natural Selection. *Statistics and Computing* 4, 2 (1994), 87–112.

[13] Vladimír Kunc and Jiří Kléma. 2024. Three Decades of Activations: A Comprehensive Survey of 400 Activation Functions for Neural Networks. *arXiv preprint arXiv:2402.09092* (2024), 109.

[14] Zachary C Lipton, David Kale, and Randall Wetzel. 2016. Directly Modeling Missing Data in Sequences with RNNs: Improved Classification of Clinical Time Series. In *Machine Learning for Healthcare Conference*. PMLR, JMLR.org, Los Angeles, California, USA, 253–270.

[15] Roderick J. A. Little and Donald B. Rubin. 2019. *Statistical Analysis with Missing Data* (2 ed.). John Wiley & Sons, Hoboken, NJ, USA.

[16] Fábio MF Lobato, Vincent W Tadesky, Igor M Araújo, and Ádamo L de Santana. 2015. An Evolutionary Missing Data Imputation Method for Pattern Classification. In *Proceedings of the Companion Publication of the 2015 Annual Conference on Genetic and Evolutionary Computation*. Association for Computing Machinery, New York, NY, USA, 1013–1019.

[17] Alfredo Nazabal, Pablo M Olmos, Zoubin Ghahramani, and Isabel Valera. 2020. Handling Incomplete Heterogeneous Data Using Vaes. *Pattern Recognition* 107 (2020), 107501.

[18] Luca Parisi, Ciprian Daniel Neagu, Narendar RaviChandran, Renfei Ma, and Felician Campean. 2024. Optimal Evolutionary Framework-Based Activation Function for Image Classification. *Knowledge-Based Systems* 299 (2024), 112025.

[19] David M. W. Powers. 2011. Evaluation: From Precision, Recall and F-Measure to ROC, Informedness, Markedness and Correlation. *Journal of Machine Learning Technologies* 2, 1 (2011), 37–63.

[20] Prajit Ramachandran, Barret Zoph, and Quoc V Le. 2017. Searching for Activation Functions. *arXiv preprint arXiv:1710.05941* (2017), 1–13.

[21] Sebastian Risi, Yujin Tang, David Ha, and Risto Miikkulainen. 2025. *Neuroevolution: Harnessing Creativity in AI Agent Design*. MIT Press, Cambridge, MA. <https://neuroevolutionbook.com>

[22] Donald B Rubin. 1976. Inference and Missing Data. *Biometrika* 63, 3 (1976), 581–592.

[23] Joseph L Schafer and John W Graham. 2002. Missing Data: Our View of the State of the Art. *Psychological Methods* 7, 2 (2002), 147.

[24] Yige Sun, Jing Li, Yifan Xu, Tingting Zhang, and Xiaofeng Wang. 2023. Deep Learning Versus Conventional Methods for Missing Data Imputation: A Review and Comparative Study. *Expert Systems with Applications* 227 (2023), 120201.

[25] Stef Van Buuren and Karin Groothuis-Oudshoorn. 2011. MICE: Multivariate Imputation by Chained Equations in R. *Journal of Statistical Software* 45 (2011), 1–67.

[26] Stef Van Buuren and Stef Van Buuren. 2012. *Flexible Imputation of Missing Data*. Vol. 10. CRC Press, Boca Raton, FL.

[27] Jinsung Yoon, James Jordon, and Mihaela Schaar. 2018. Gain: Missing Data Imputation using Generative Adversarial Nets. In *International Conference on Machine Learning*. PMLR, PMLR, Stockholm, Sweden, 5689–5698.